

# Characterization of a $\delta/\gamma$ duplex stainless steel

J. A. JIMENEZ, M. CARSI, O. A. RUANO

*Department of Physical Metallurgy, Centro Nacional de Investigaciones Metalúrgicas, C.S.I.C., Avda. Gregorio del Amo 8, 28040 Madrid, Spain*  
*E-mail: jimenez@cenim.csic.es*

F. PEÑALBA

*INASMET, Camino de Portuete 12, 20009 San Sebastián, Spain*

A duplex stainless steel was investigated in both as-received sheet and after annealing at temperatures ranging from 850 to 1100°C. The sheet presents a deformation texture in both phases, austenite and ferrite, induced by cold rolling. Microstructure in the as-received material consists of island-like austenitic grains in a ferrite matrix. These austenitic grains are elongated with an average size of 6, 20 and 40  $\mu\text{m}$  along the normal (ND), transversal (TD) and rolling direction (RD). Quantitative texture measurements demonstrated that texture components are distributed mainly along the  $\theta$ -fiber (ND  $\parallel$   $\langle 100 \rangle$ ) and  $\alpha$ -fiber (RD  $\parallel$   $\langle 110 \rangle$ ) for the ferrite and the  $\zeta$ -fiber (ND  $\parallel$   $\langle 110 \rangle$ ) for the austenite. After recrystallization, a decrease in the intensity of the mean fibers and an increase in the minor components was observed in both, ferrite and austenite. Therefore, a similar texture was reached in both phases after annealing at 1050°C. Microstructural characterization after annealing at temperatures above 850°C showed that the elongated austenitic grains transform in colonies of equiaxed grains of about 10–15  $\mu\text{m}$  in size. These colonies are surrounded by a ferritic matrix at annealing temperatures above 1000°C or by a laminar microstructure at temperatures below 950°C. This laminar microstructure includes sigma phase and austenite formed from delta ferrite, and untransformed delta ferrite. © 2000 Kluwer Academic Publishers

## 1. Introduction

Duplex stainless steels have been used in many diverse fields like ship construction or chemical industry. The large applications of these steels are related to their excellent resistance to corrosion and stress-corrosion, as well as a high strength combined with high toughness [1, 2]. The good mechanical properties of these steels are due to the duplex structure of ferrite ( $\delta$ ) and austenite ( $\gamma$ ): in one part the ferrite is responsible of the strength, and in the other, the austenite ensures the toughness of the material [3]. The exact amount of each phase present in the microstructure can be deduced in terms of the amount of the principal alloying elements (chromium and nickel). Concentration of these elements is adjusted using the ternary Fe-Ni-Cr equilibrium diagram to obtain a microstructure consisting of about the same amount of ferrite and austenite. In addition to chromium and nickel, other alloying elements like nitrogen, molybdenum, copper, silicon, manganese, and tungsten may be added to control structural balance and to improve corrosion-resistance characteristics [4].

Conventional duplex stainless steels contain Cr (21–23 wt. %), Ni (4.5–6.5 wt. %) and Mo (about 3%) [4]. These steels are capable of forming  $\sigma$  phase during prolonged exposure to temperatures ranging from 450–900°C [5, 6]. The  $\sigma$  phase is a hard, brittle, and non

magnetic intermetallic phase with a tetragonal crystal structure. The temperature at which it can form is a function of the composition of the steel, the plastic deformation and the prior thermal history [7–13]. In  $\delta$ – $\gamma$  duplex stainless steels,  $\sigma$  phase particles normally nucleate at ferrite-austenite interphase boundaries and grow into the adjacent ferrite grains in the form of a cellular structure consisting of  $\sigma$  phase and new austenite at temperatures between 675 and 975°C [14, 15]. Precipitation of  $\sigma$  phase in duplex stainless steels containing relatively high Cr and low Ni concentrations is much faster than that in austenitic or ferritic steels, and can occur during cooling in the production process. Thus, it is common to quench the steel after solution treatment at high temperature in order to avoid the presence of sigma phase.

The presence of a fine-grained microstructure generally yields to an improvement of the mechanical properties of duplex stainless steels. Grain refinement is usually obtained in the as-casted material by means of an adequate thermomechanical process. Such process, which consists conventionally in hot and/or cold rolling of the material, determines the development of a crystallographic texture. Texture is one of the factors that affects anisotropy of the mechanical properties of steel sheets. However, systematic investigations have not been carried to study the influence of both phases,

ferrite and austenite, on the formation of the recrystallization texture. The present investigation is aimed to study the microstructure including texture of a commercial duplex stainless steel. The effect of annealing temperature in the range from 850 to 1100°C on the microstructure and texture evolution is also investigated.

## 2. Experimental procedure

The material used in this study has the nominal composition (in weight %) Fe-22.5 Cr-6.0 Ni-3.0 Mo-0.6 Si-1.4 Mn. The material was supplied as a sheet of 3 mm in thickness prepared by hot forging ingots and a further cold rolling reduction of about 50%.

The microstructure of the as-received alloy, and that after annealing at temperatures ranging from 850 to 1100°C for 1.5 h were characterized using various techniques including X-ray diffraction, optical microscopy, and scanning electron microscopy (SEM) equipped with energy dispersive X-ray microanalysis.

Identification of the present phases, lattice parameter measurements, and determination of the volume fraction of each phase was conducted by X-ray analysis [5, 6]. The diffraction studies were performed employing Cu  $K_{\alpha}$  radiation. Automatic step scanning allowed the accumulation of a sufficient number of counts at each Bragg angle to obtain the desired statistical accuracy. Lattice parameters of  $\delta$ ,  $\gamma$ , and  $\sigma$  phases were calculated by least squares and they were reproducible within 0.0001 nm. The main difficulty in quantification of the X-ray diffraction peaks intensities of each phase arises from the overlapping of diffraction peaks (330) of the  $\sigma$  phase with the (111) peaks of the  $\gamma$  phase, and also the (202) peaks of the  $\sigma$  phase with the (110) peaks of the  $\delta$  phase. Thus, the volume fraction of each phase was calculated from the integrated intensities of (002), (410), (212), (411), (331), (222) and (132)  $\sigma$  phase peaks, (200), (211), (220) and (310) ferrite peaks and (200), (220), (113), (222) and (400) austenite peaks [7].

Texture measurements were carried out by means of the Schulz reflection method in the as-received material and after annealing at 1050°C. Overlapping of diffraction peaks of the  $\sigma$  phase with some of the peaks of the  $\delta$  and  $\gamma$  phase did not allow to extend this analysis to the samples annealed at temperatures below 950°C. Details of the diffractometer used and the analysis method are given elsewhere [16]. The orientation distribution function, ODF, not only allows the determination of the different texture components, but also the calculation of the volume fraction,  $F_v$ , associated with each one. In this work,  $F_v$  was calculated by a numerical integration method from the ODF intensity data [17]. As integration limits for this calculation, orientations 10° apart from the ideal orientation have been considered to belong to a given fiber.

The microstructures of samples were examined by both optical and scanning electron microscopy, SEM. Metallographic preparation included mounting the samples in bakelite and polishing by the conventional method. The microstructure was revealed by chemical etching with a solution of 15 ml HNO<sub>3</sub> and 30 ml HCl on the  $\delta$ -ferrite/austenite duplex microstruc-

ture and by a solution of 0.5 g K<sub>2</sub>S<sub>2</sub>O<sub>5</sub>, 10 ml HCl and 50 ml H<sub>2</sub>O when the  $\sigma$  phase was present.

The distribution of alloying elements in the various phases after annealing at different temperatures was examined by microanalysis with an energy dispersive X-rays spectrometer, EDX. Semiquantitative analysis

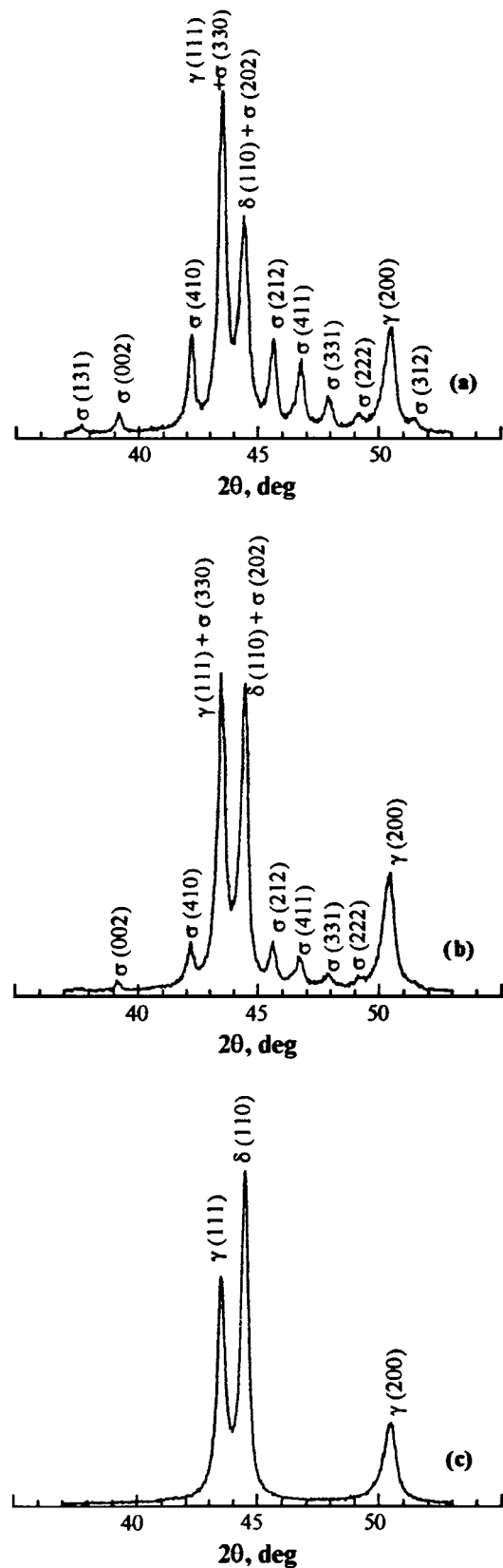


Figure 1 X-ray diffraction patterns of duplex stainless steel after annealing for 1.5 h at (a) 850, (b) 950 and (c) 1050°C.

of all the present phases in the microstructure was only performed in the as-received samples and after annealing at temperatures above 950°C. For samples treated at lower temperatures, semiquantitative analysis was only performed in the austenitic grains grouped in colonies. This is because the phases present in the laminar structure were smaller than the excitation area from the electron beam, so accurate analyses would not be possible.

### 3. Results

#### 3.1. X-ray diffraction

The X-ray diffraction pattern of duplex stainless steel in the as-received sheet shows the presence of two phases:  $\delta$ -ferrite and  $\gamma$ -austenite. Compared to the theoretical intensities of  $\delta$ -ferrite and  $\gamma$ -austenite, enhanced intensity of the (200) peak of ferrite and (220) peak of austenite was found. This suggests that a texture is de-

veloped in the grains of both phases during cold rolling of ingots into thick plates.

The diffraction patterns of the samples annealed in the temperature range from 800 to 900°C are similar and showed the presence of three phases:  $\delta$ -ferrite,  $\gamma$ -austenite and  $\sigma$  phase. The sigma phase was also present in the samples annealed at 950°C but with a lower intensity. This phase was not detected after annealing at temperatures above 1000°C. Fig. 1a, b and c show the diffraction patterns of samples annealed at 850, 950 and 1050°C respectively. A relationship between the intensity of the peaks corresponding to  $\delta$ -ferrite and  $\sigma$  phase is observed in these diagrams. The higher are the  $\sigma$  phase diffraction peaks, the lower are the ferrite peaks. On the other hand, the difference in the intensity of the austenitic peaks for the various annealings was not so pronounced.

Fig. 2 shows the volume fraction changes of each phase after annealing for 1.5 h at different temperatures. An increase in the volume fraction of the  $\sigma$  phase is accompanied by a decrease of the  $\alpha$  phase, while the amount of austenite was estimated to be about 45% in volume independently of the annealing temperature.

The broad diffraction peaks present in the diffraction pattern of the as-received sheet sharpen after annealing for 1.5 h at temperatures ranging from 800 to 1100°C. This effect can be attributed to a recrystallization process. The diffraction peaks corresponding to the ferrite and austenite occupy the same position in the as-cast and annealed materials. Thus, the values of the lattice parameter deduced by the least squares method did not depend on the annealing temperature. Values of 0.3608 nm for the austenite and 0.2882 nm for the ferrite were obtained. For the  $\sigma$  phase, the value for the  $a$  and  $c$  axis measured were 0.8833 and 0.46061 nm, respectively.

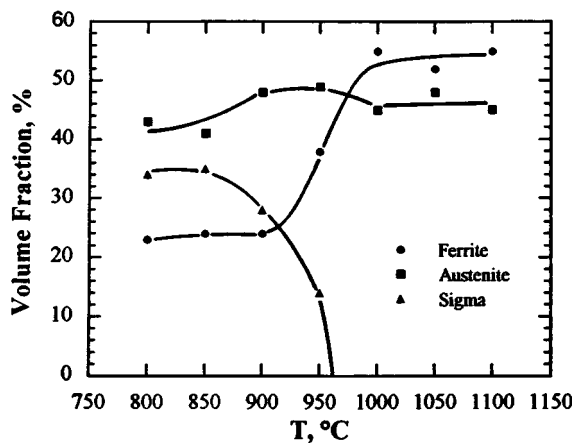


Figure 2 Volume fraction changes of  $\alpha$ ,  $\gamma$ , and  $\sigma$  phases after annealing for 1.5 h at different temperatures.

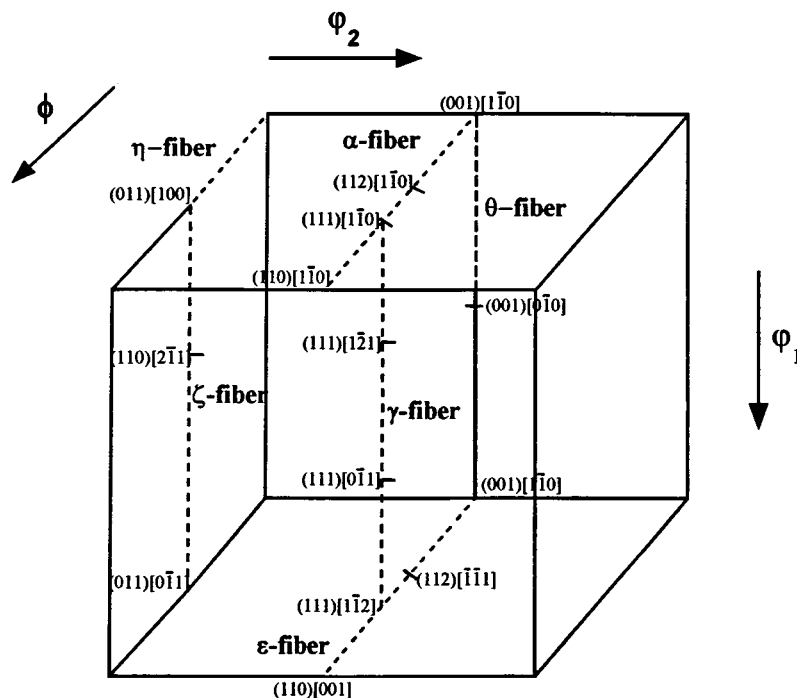


Figure 3 Schematic representation of the most important fiber textures in the three dimensional Euler angle space.

### 3.2. Texture

The texture analysis was performed by means of the ODF. As both phases ferrite and austenite present a cubic crystal symmetry, the orientation density,  $f(g)$ , was represented in the reduced Euler space ( $0 \leq \varphi_1, \phi, \varphi_2 \leq \pi/2$ ). The rolling texture components in steels concentrate along fibers, which are defined by an orientation rotated around a given axis. The most important fibers are schematically represented in the three dimensional Euler angle space in Fig. 3.

Complete experimental ODFs of ferrite and austenite cold rolling texture are presented in Fig. 4a and b at

$\varphi_1$ -sections through the Euler space. According to the scheme of Fig. 3, it can be concluded that the texture components developed during cold rolling (and thus after annealing) of the duplex stainless steel are distributed mainly along four fibers:  $\theta$ -fiber (ND  $\parallel$  (100)),  $\alpha$ -fiber (RD  $\parallel$  (110)),  $\zeta$ -fiber (ND  $\parallel$  (110)) and a weak  $\gamma$ -fiber (ND  $\parallel$  (111)), where RD is the rolling direction and ND is the direction parallel to the sheet normal.

In order to show in more detail the changes in texture in the material after annealing, the orientation density along these four fibers is given in Fig. 5a to d for both

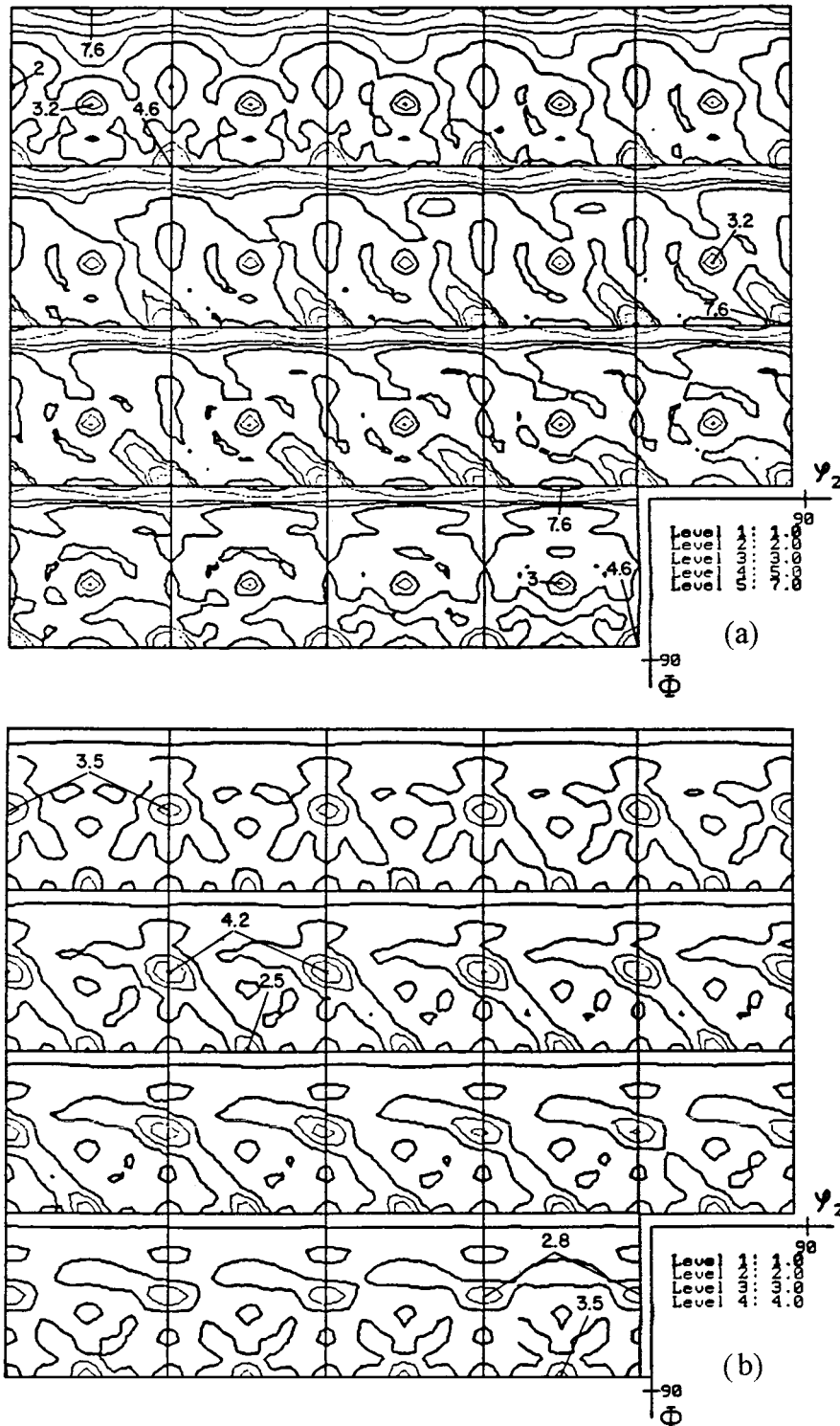


Figure 4 Complete experimental ODFs of (a) ferrite and (b) austenite in the as-received material.

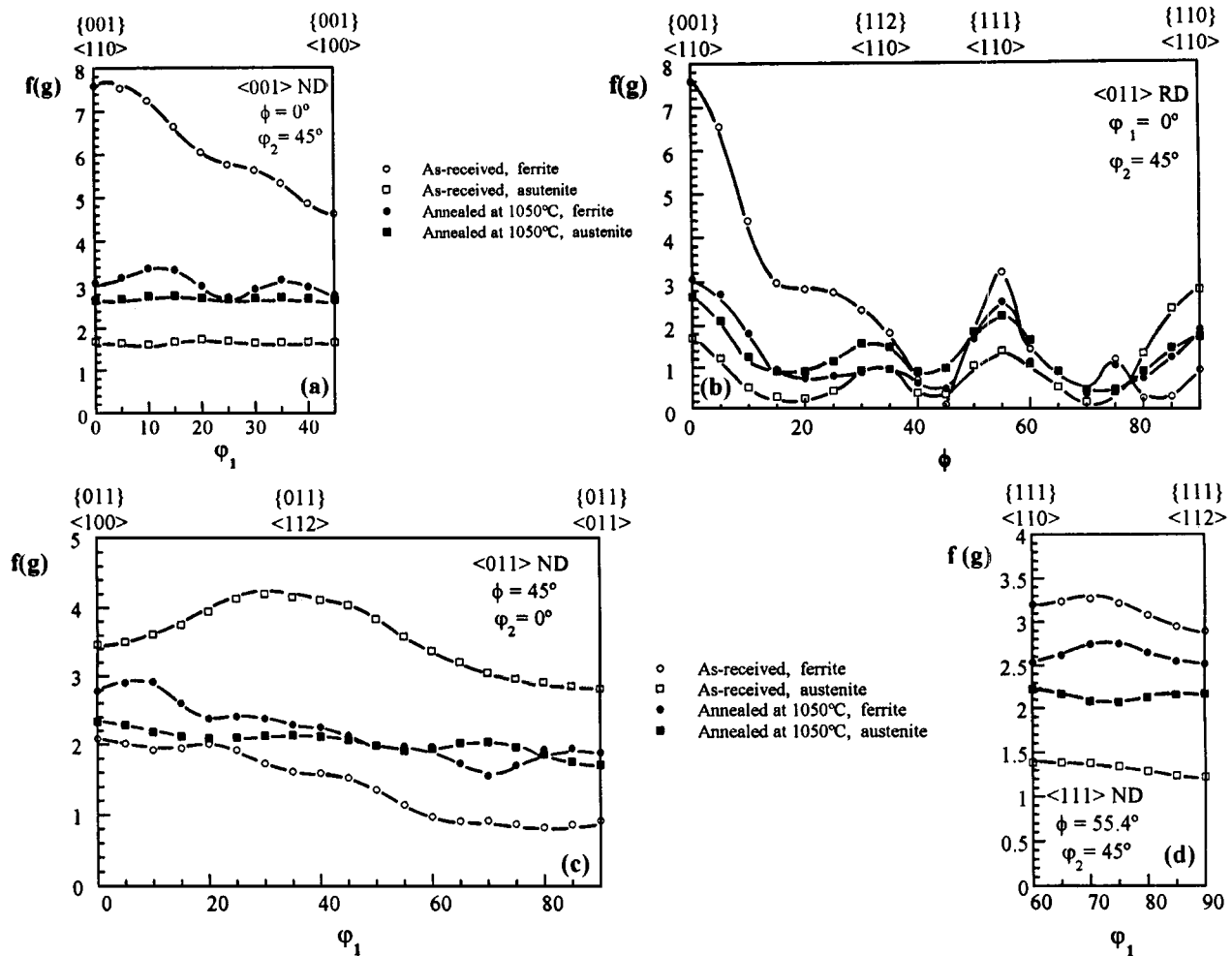


Figure 5 Orientation density along the (a)  $\theta$ -fiber, (b)  $\alpha$ -fiber, (c)  $\zeta$ -fiber, and (d)  $\gamma$ -fiber in the as received and the annealed materials.

phases austenite and ferrite. In the case of the ferrite these plots show:

1. A marked decrease in the intensity of the  $\theta$ -fiber after annealing (Fig. 5a). Thus, the volume fraction of crystallites belonging to this fiber calculated from the ODF decreased from 35% in the as-received material to 20% after annealing at 1050°C for 1.5 h.

2. A decrease after annealing in the relative orientation density difference between  $\{001\}\langle 110 \rangle$  and  $\{112\}\langle 110 \rangle$  on the  $\alpha$ -fiber, while the component  $\{111\}\langle 110 \rangle$  remains practically constant (Fig. 5b). In this case, the volume fraction of crystallites belonging to this fiber decreased from 27% in the as-received material to 19% after annealing at 1050°C for 1.5 h.

3. An increase in the density of all the orientations included on the  $\zeta$ -fiber, remaining in the annealed material a weak preference for the Goss component,  $\{110\}\langle 001 \rangle$  (Fig. 5c). The volume fraction of this fiber increases from 12% in the as-received material to 18% after annealing at 1050°C for 1.5 h.

4. The orientation density along the  $\gamma$ -fiber is hardly affected by the annealing at 1050°C for 1.5 h (Fig. 5d). This texture is the weakest with a volume fraction of 4 and 3.5% in the as received and the annealed materials, respectively.

On the other hand, as shown in Fig. 5a to d, the cold rolling texture in the austenite reveals a very different

feature: the formation of a strong  $\zeta$ -fiber, for which the mean component is the brass component ( $\{011\}\langle 112 \rangle$  in Fig. 5c). After annealing at 1050°C, the volume fraction of the  $\zeta$ -fiber decreases (from 24 to 15%), while increasing the intensity of the other three fibers ( $\theta$ -fiber from 10 to 18%,  $\alpha$ -fiber from 14 to 19%, and  $\gamma$ -fiber from 2 to 3%).

### 3.3. Microstructure

The microstructural features of duplex stainless steels observed are significantly influenced by thermomechanical processing routes and additional annealing. Microstructure of the as-received material consists of a duplex  $\delta$ - $\gamma$  microstructure, with island-like austenitic grains in a more or less continuous matrix of ferrite, as is shown in Fig. 6. These austenitic grains are elongated with an average size of 6, 20 and 40  $\mu\text{m}$  along the normal, transversal and rolling direction, respectively.

During annealing at 850°C, a recrystallization of the material occurs, as observed in Fig. 7a. This figure shows a fine microstructure consisting of austenitic grains of about 10  $\mu\text{m}$  grouped in colonies, surrounded by a lamellar microstructure. This figure also shows the presence of small particles along the austenitic grain boundaries. Qualitative microanalysis of these particles by EDXS shows a high level of Cr and Mo, characteristic of the  $\sigma$  phase. On the other hand, the lamellar structure is constituted by particles of  $\sigma$  phase, not dissolved

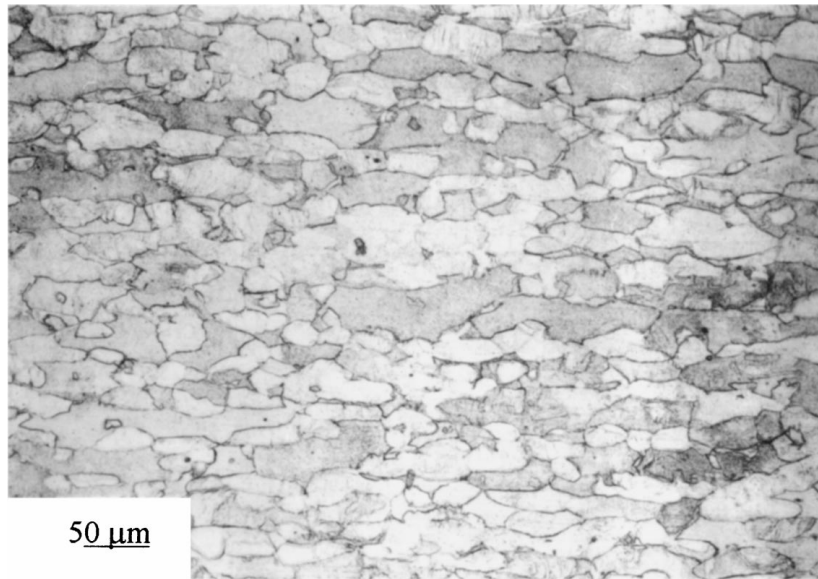


Figure 6 Typical microstructure of the as-received material.

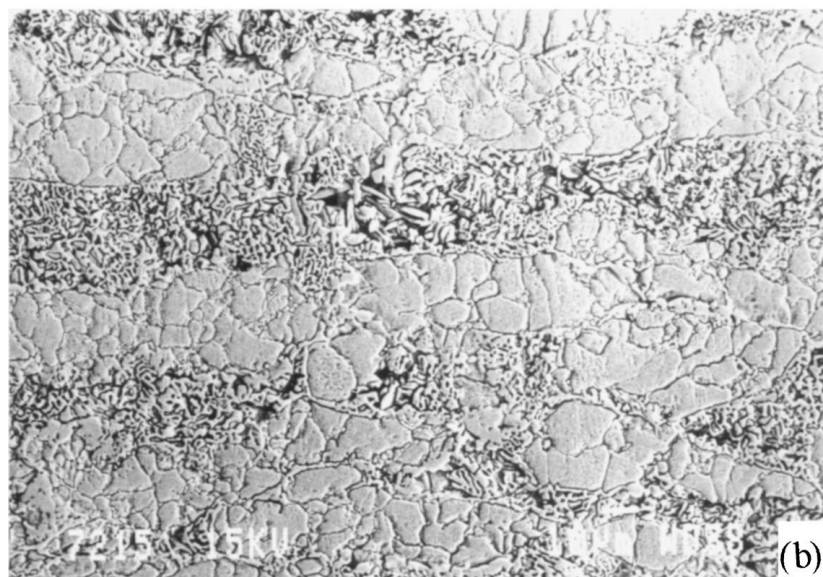
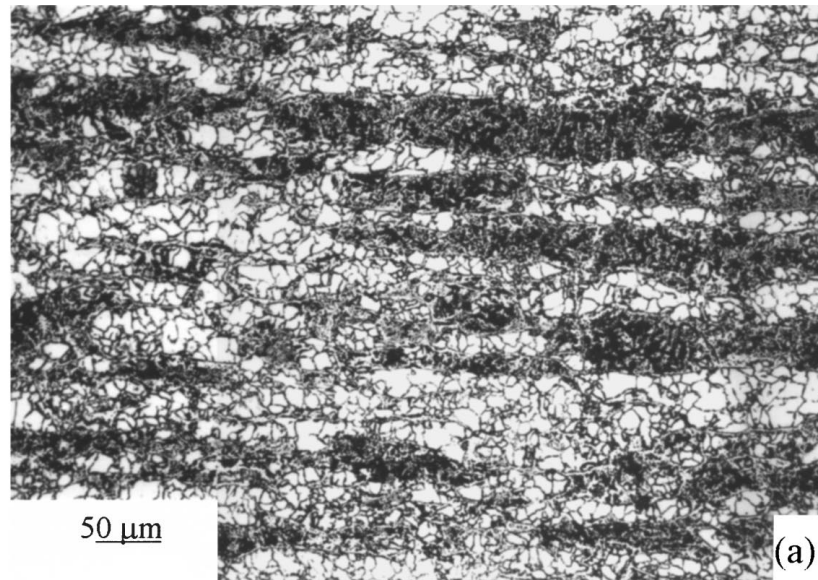


Figure 7 Microstructure after annealing for 1.5 h at 850°C: (a) Optical and (b) SEM micrographs.

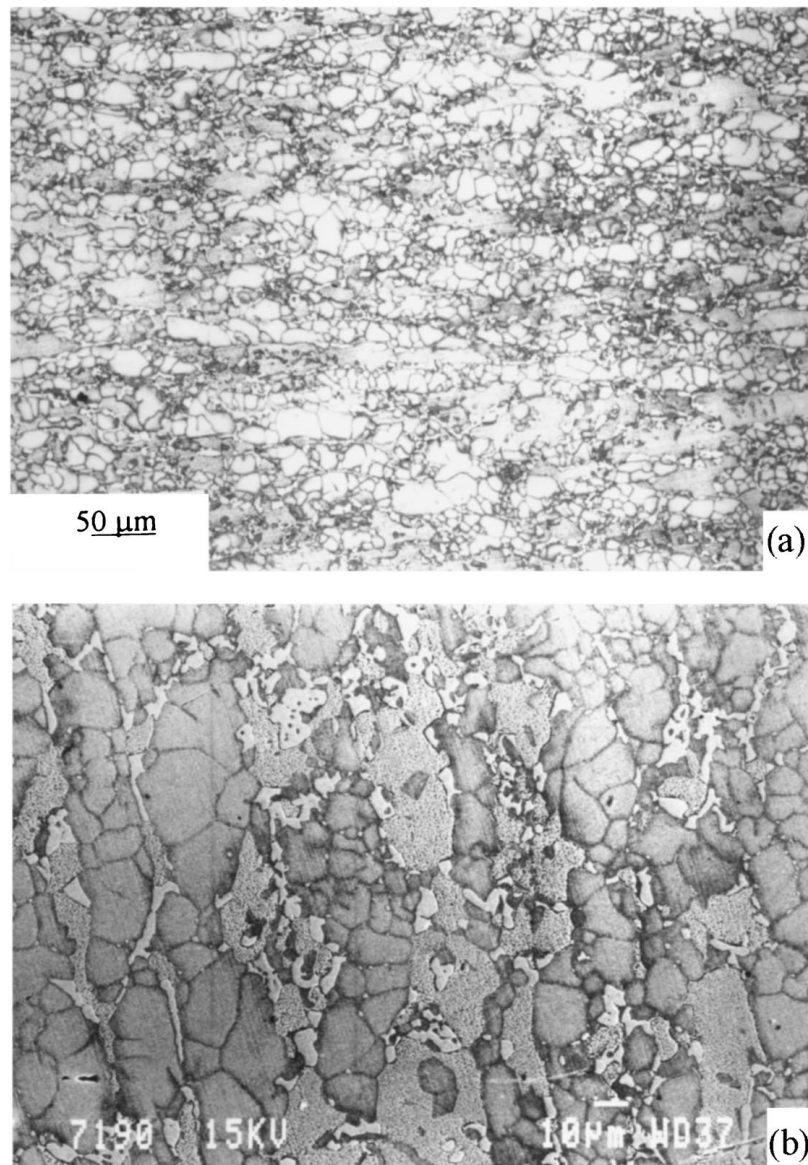


Figure 8 Microstructure after annealing for 1.5 h at 950°C: (a) Optical and (b) SEM micrographs.

by the etching used, and new austenite phase. A detail of this microstructure is presented in Fig. 7b. In addition to the  $\sigma$  phase, the existence of some amount of delta ferrite grains in such lamella was confirmed by X-ray diffraction, as shown in Fig. 1a. However, it was impossible to discriminate the phases by SEM because of their small size.

The microstructure of the material after annealing at 950°C is presented in Fig. 8a and b. Although the existence of a structure consisting of  $\delta$ ,  $\gamma$  and  $\sigma$  phases was confirmed by X-ray diffraction, the microstructure differs from that presented in Fig. 7. As for the material annealed at 850°C, small austenite grains are grouped in coarse islands formed during the solution treatment. However, the microstructure of the matrix phase is completely different. At this annealing temperature, a higher volume fraction of retained delta ferrite is observed in the place occupied by the laminar structure in Fig. 7a and b. The sigma phase is mostly placed at the primitive ferrite/austenite interphase of the as-received material, but also some small amount of sigma particles are observed along the austenitic grain boundaries.

Furthermore, some isolated austenitic grains inside the untransformed delta-ferrite are also observed in Fig. 8b.

The microstructure after annealing at 1050°C for 1.5 h is presented in Fig. 9a and b. The figure shows a binary microduplex microstructure consisting of austenitic grains of about 15  $\mu\text{m}$  grouped in colonies in a matrix of ferrite grains. As in austenitic stainless steels, the austenitic grains usually present twins.

The partitioning of the alloying elements in the phases was analyzed by EDXS in the as-received material, as well as after annealing at 950 and 1050°C. The results are summarized in Table I. This table shows only small differences in the composition of the ferrite and the austenite after annealing at both temperatures. It is worth noting the high concentration of Ni in austenite and of Cr and Mo in the  $\sigma$  phase.

#### 4. Discussion

Texture analysis and metallographic studies of the  $\delta$ -ferrite/austenite duplex stainless steel in the as-received material and after annealing for 1.5 hours at

TABLE 1 Microanalysis results in weight per cent of the phases present in the duplex stainless steel in the as-received condition and after annealing at 950 and 1050°C for 1.5 h

	Fe	Cr	Ni	Mo	Mn	Si
As received						
Ferrite	65 ± 1	24 ± 1	5.1 ± 0.2	3.3 ± 0.2	1.5 ± 0.2	1.1 ± 0.1
Austenite	66 ± 1	22 ± 1	7.0 ± 0.2	2.1 ± 0.2	1.7 ± 0.2	1.2 ± 0.1
Annealed at 950°C						
Ferrite	65 ± 1	24 ± 1	4.7 ± 0.2	3.4 ± 0.2	1.5 ± 0.2	1.4 ± 0.1
Austenite	66 ± 1	22 ± 1	6.9 ± 0.2	2.3 ± 0.2	1.7 ± 0.2	1.1 ± 0.1
σ Phase	56 ± 1	30 ± 1	3.3 ± 0.3	8.2 ± 1	1.5 ± 0.2	1.0 ± 0.1
Annealed at 1050°C						
Ferrite	64 ± 1	25 ± 1	5.0 ± 0.2	3.3 ± 0.2	1.5 ± 0.2	1.2 ± 0.1
Austenite	66 ± 1	22 ± 1	7.1 ± 0.2	2.2 ± 0.2	1.7 ± 0.2	1.1 ± 0.1

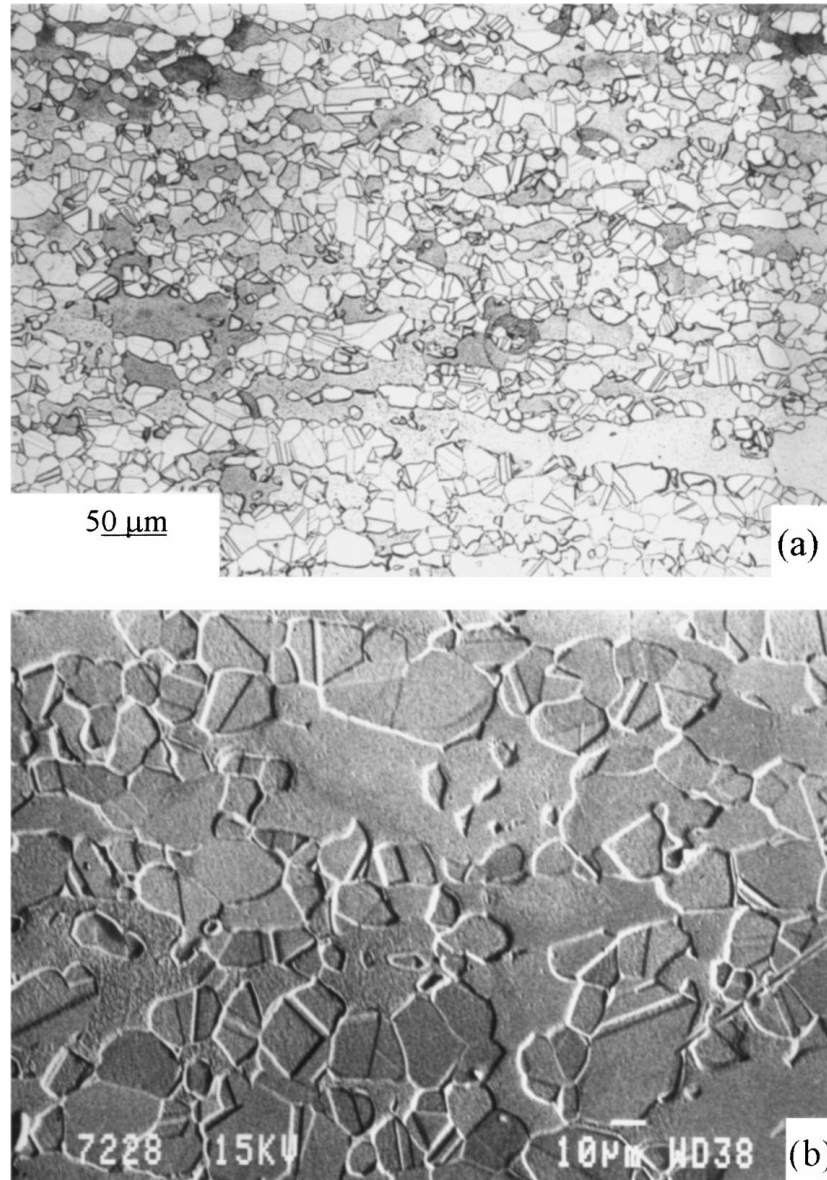


Figure 9 Microstructure after annealing for 1.5 h at 1050°C: (a) Optical and (b) SEM micrographs.

temperatures above 850°C indicate the existence of static recrystallization. After a cold rolling reduction of about 50% at room temperature the microstructure of the sheet consists of austenitic island-like grains in a ferritic matrix. These austenitic grains lay elongated in the rolling direction, and a strong texture is observed in both, austenite and ferrite. After annealing at temperatures above 850°C, the orientation density of the strong rolling components decrease as observed in Fig. 5. This

change in the texture is a consequence of recrystallization during annealing as confirmed metallographically. As shown in Figs 7–9, these elongated austenitic grains transform to colonies of equiaxial small grains lower than 15 μm in size, to form the final microduplex microstructure.

The present study shows that the texture found in the ferrite is different from that found in other ferritic steels containing a high amount of Cr (up to 17 wt%), where

the main component are the  $\alpha$ - and  $\gamma$ -fibers [18]. As shown in Fig. 5a and b, the dominant texture components in the ferrite are located in the  $\theta$ - and  $\alpha$ -fiber, with a volume fraction of grains belonging to these fibers of 35 and 27%, respectively. These initial strong components decreased after recrystallization to a volume fraction of 20 and 19%, respectively. At the same time the volume fraction of the  $\zeta$ -fiber increased from 12 to 18% after annealing for 1.5 h at 1050°C. Although these values would indicate the presence of a strong texture in the annealed material, an integration of the ODF for a random oriented material between the same limits used for these calculations led to values of the volume fractions of 10, 12 and 15% for the  $\theta$ -,  $\zeta$ -, and  $\alpha$ -fiber, respectively. This corresponds to a weak texture of the annealed material.

On the other hand, the main components of the rolling texture of austenite are distributed along the  $\zeta$ -fiber. This fiber constitutes one of the two fibers experimentally found in FCC metals after rolling [19]. After recrystallization, the mean component of the fiber, which is the brass component  $\{011\}\langle 112\rangle$ , disappears, as observed in Fig. 5c. Thus, the texture of both, ferrite and austenite, is similar after annealing at 1050°C.

Precipitation of the  $\sigma$  phase during annealing at temperatures up to 950°C has been confirmed by X-ray diffraction (Fig. 1) and metallographic studies (Figs 7 and 8). Although this phase can be formed from both ferrite and austenite, Figs 7 and 8 show low volume fraction particles of  $\sigma$  phase included in the colonies of grains of austenite. Thus, the  $\sigma$  phase is mainly formed from ferrite, and consequently the intensity of diffraction peaks of ferrite in Fig. 1 decreases when the  $\sigma$  phase appears.

On the other hand, Fig. 7 shows that the ferrite grains transform to a laminar structure consisting of ferrite,  $\sigma$  phase and austenite. This laminar structure has been explained in previous investigations as the result of the eutectoid decomposition of  $\delta$ -ferrite into  $\sigma$  phase and austenite [14, 20]. However, the X-ray diffraction patterns of the samples annealed at temperatures below 950°C indicate the presence of a high volume fraction of non-transformed ferrite (about 24%) and a volume fraction of austenite similar to that for the as-received material. Another interpretation for the microstructural evolution of ferrite, therefore, can be made by considering the precipitation of austenite and  $\sigma$  phase to occur in two steps. In a first step, the  $\sigma$  phase would precipitate from ferrite. Since the  $\sigma$  phase contains a high concentration of chromium and molybdenum, the precipitation of a high volume fraction of this phase (about 34 vol%) should enrich the residual ferrite with iron and nickel. Thus, additional precipitation of some austenite can be produced from the ferrite.

## 5. Conclusions

1. Duplex stainless steel in the as-received sheet shows a microstructure of austenitic grains elongated along the rolling direction in a ferrite matrix.

2. Recrystallization of the material occurs after annealing at temperatures above 850°C. Elongated grains

of austenite transform into colonies of fine and equiaxed grains of 10 to 15  $\mu\text{m}$  in size. On the other hand, precipitation of sigma phase particles at grain boundaries is observed at annealing temperatures up to 950°C.

3. Delta ferrite islands transform to a laminar structure consisting of ferrite, austenite and  $\sigma$  phase during annealing at temperatures below 950°C. The formation of sigma phase and austenite from ferrite occurs in two steps. First a precipitation of the  $\sigma$  phase occurs, and then the austenite can be formed from the iron and nickel enriched ferrite.

4. Texture components developed during the rolling process are distributed mainly along the  $\theta$ -fiber (ND  $\parallel$   $\langle 100\rangle$ ) and the  $\alpha$ -fiber (RD  $\parallel$   $\langle 110\rangle$ ) for the ferrite and the  $\zeta$ -fiber (ND  $\parallel$   $\langle 110\rangle$ ) for the austenite. After recrystallization, a decrease in the intensity of the mean fibers and an increase of the minor components was observed in both, ferrite and austenite. Therefore, a similar weak texture was reached in both phases after annealing at 1050°C.

## Acknowledgements

This work was sponsored by the Comisión Interministerial de Ciencia y Tecnología (CICYT) under Grant MAT 97/0700.

## References

1. R. G. GIBSON, H. W. HAYDEN and J. H. BROPHY, *Trans. ASM* **61** (1968) 85.
2. H. W. HAYDEN and S. FLOREEN, *ibid.* **61** (1968) 474.
3. S. FLOREEN and H. W. HAYDEN, *ibid.* **61** (1968) 489.
4. K. FORCH, C. GILLESSEN, I. VON HAGEN and W. WEBLING, *Stahl und Eisen* **112** (1992) 53.
5. J. I. MORLEY and H. W. KIRKBY, *J. Iron Steel Inst.* **172** (1952) 129.
6. Y. MAEHARA, Y. OHMORI and T. KUNITAKE, *Met. Technol.* **10** (1983) 296.
7. J. V. HARDY and G. T. BROWN, *J. Iron Steel Inst.* **202** (1964) 437.
8. A. J. COOK and B. R. BROWN, *ibid.* **171** (1952) 345.
9. R. BLOWER and G. J. COX, *ibid.* **208** (1970) 769.
10. M. LEWIS, *Acta Metall.* **14** (1966) 1421.
11. R. J. GRAY, V. K. SIKKA and R. J. KING, *J. Met.* **30** (1978) 18.
12. B. WEISS and R. STICKLER, *Metall. Trans.* **3** (1972) 851.
13. R. G. ELLIS and G. POLLARD, *J. Iron Steel Inst.* **208** (1970) 783.
14. Y. MAEHARA, Y. OHMORI, J. MURAYAMA, N. FUJINO and T. KUNITAKE, *Met. Sci.* **17** (1983) 541.
15. Y. MAEHARA and Y. OHMORI, *Metall. Trans.* **18** (1987) 663.
16. M. T. PEREZ-PRADO, J. IBAÑEZ, M. MORRIS, M. C. CRISTINA, O. A. RUANO and G. GONZALEZ-DONCEL, *Rev. Metal. Madrid* **34** (1998) 324.
17. M. J. CAI and W. B. LEE, in "Proc. 10th Int. Conf. Textures of Materials," Clausthal, Germany, 1993, edited by H. J. Bunge, *Materials Science Forum* **157-162** (1994) 327.
18. D. RAABE and K. LÜCKE, in "Proc. 10th Int. Conf. Textures of Materials," Clausthal, Germany, 1993, edited by H. J. Bunge, *Materials Science Forum* **157-162** (1994) 597.
19. J. HIRSCH and K. LÜCKE, *Acta Metall.* **36** (1988) 2863.
20. Y. MAEHARA, M. KOIKE, N. FUJINO and T. KUNITAKE, *Trans. Iron Steel Inst. Jpn.* **23** (1983) 240.

Received 28 January  
and accepted 11 August 1999